

# Evaluation of the Most Suitable Hyperchaotic Map in S-Box Design Used in Image Encryption

Hala Saeed<sup>1</sup>, Hossam E.Ahmed<sup>2</sup>, Tamer O.Diab<sup>3</sup>, Hossam L.Zayed<sup>4</sup>, Hany Nasry Zaky<sup>5</sup>,  
Wageda I.Elsobky<sup>6</sup>

<sup>1</sup>Department of Basic Sciences, Benha Faculty of Engineering, Benha University, Egypt

<sup>2</sup>Department of Electrical Engineering- Benha Faculty of Engineering, Benha University, Egypt

<sup>3</sup>Department of Electrical Engineering- Benha Faculty of Engineering, Benha University, Egypt

<sup>4</sup>Department of Electrical Engineering- Benha Faculty of Engineering, Benha University, Egypt

<sup>5</sup>Department of Mathematics, Military Technical College, Egypt

<sup>6</sup>Department of Basic Sciences, Benha Faculty of Engineering, Benha University, Egypt

Email address: <sup>1</sup>hala.saeed@bhit.bu.edu.eg, <sup>2</sup>hossameldin.ibrahim@bhit.bu.edu.eg, <sup>3</sup>tamer.almarsafawy@bhit.bu.edu.eg,

<sup>4</sup>hossam.zayed@bhit.bu.edu.eg, <sup>5</sup>hanynasry@mtc.edu.eg, <sup>6</sup>wageda.alsobky@bhit.bu.edu.eg

**Abstract**— This research presents a survey of application of hyperchaotic map on encryption of color images. There are various researches that have introduced this application. Among these papers, one of them has presented a technique for altering and encoding color images based on S-box based on the hyperchaotic map foundation and several chaotic maps and an. It has shown its efficiency against a wide range of cryptographic assaults and has obtained good results.

**Keywords**— Hyperchaotic map; Image encryption; S-box.

## I. INTRODUCTION

A chaotic map is a map (specifically, an evolution function) that demonstrates some type of randomness in mathematics. Henri Poincaré was an early proponent of chaos theory. While examining the three-body problem in the 1880s, he observed that there can be non-periodic orbits that are neither forever rising nor nearing a fixed point. [1]. The continual recurrence of simple mathematical formulas has been central to most of chaos theory's mathematics. Until now, chaotic maps had been in constant evolution. They've worked on a variety of applications, including encryption, robotics, biology, and economics [2-4]. Chaos in one-dimensional (1D) and high-dimensional (HD) dimensions are two types of chaotic systems that have been a widely researched issue for academics. Classical 1D chaotic systems include the logistic, sine, and tent maps [5,34]. The chaotic sequences created by 1D chaotic maps are less stochastic and pose a number of security problems in visual encryption processing due to their low complexity and predictability [6-8]. The behaviour of chaotic sequences is more difficult to anticipate and more suitable for visual encryption theoretically in HD chaotic systems, which have a bigger parameter space and more complicated structure than 1D chaotic systems. To strengthen the security and performance analysis of the cryptographic algorithms, multiple hybrid chaotic maps have been presented to be utilized in image encryption [9]. This paper introduces a survey of some work that has employed the hyperchaotic maps in image encryption. One of these papers has presented image encryption scheme that achieved good outcomes between

others [10]. That study developed a two-level approach for altering data of color image. The first seeks to change the placements of bits within data of the pixel, while the second uses the S-box to change the placements of pixels in the plain photo. The encrypting stage is timed to coincide with the development of two chaos maps of less mathematical complexity, the 1D logistic map [11] and the 3D Hénon map [12,13], which have fused to generate hybrid chaos split into three matrices. Each of these matrices creates the encrypted image when the low-complexity XOR operation is carried out between the photo data collected by the altering stage and the information of the matrix supplied by the hybrid chaos producer. The remainder of the study is organized as follows: The majority of relevant work has been introduced in section 2. The maps that were used are explained in section 3. The most suitable scheme has been illustrated in section 4. The experimental results of this scheme are presented in section 5.

## II. RELATED WORK

Color images give important information than grey images, hence different algorithms for encoding them are discussed. Employing a hyperchaotic Lorenz system that is paired, Kadir et al. [14] suggested a new approach for encrypting colored images, but the encryption algorithm was easy. Irani et al. [15] proposed a new chaotic map in one-dimension for encoding color images called a chaotic coupled Sine map. Liu et al. [16] suggested a novel 2D Chebyshev-Sine map for color image encryption and implemented it. The map was utilized to construct three sequences that were used to disperse the three channels. Nevertheless, the algorithm is solely based on diffusion. A new encoding for color image technique is proposed [17], which is relied on non-uniform cellular automata and a hybrid hyper-chaotic system. Implementing two identical one-dimensional (1D) chaotic maps, Pak and Huang [18] proposed a new chaotic system. The system is then used to encrypt color images both in confusion and diffusion steps. Article [19] was proposed to use a color picture encoding methodology that alters (permutes) and diffuses the pixels (JPD). Virtually Encryption

techniques have been built utilizing generated chains from 4D hyperchaotic systems exhibiting positive Lyapunov exponents.

III. MATH LOGISTIC MAP, ZASLAVASKY MAP AND 3D AND HÉNON MAP

In the image encoding system described in this paper, the following maps were used:

A. Logistic map [10]

The logistic map is defined by the following formula:

$$X_{n+1} = \partial X_n(1 - X_n), \tag{1}$$

The logistic parameter is noted as  $\partial \in [0,4]$ , and the logistic map operates in a chaotic state, presenting a chaotic sequence when  $\partial \in [3.569946,4]$

The phase diagram of the logistic map is shown in Fig. 1

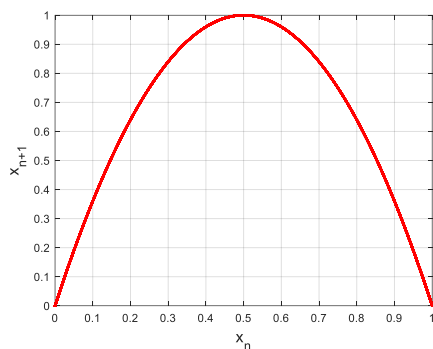


Fig. 1. Logistic map phase diagram

B. Zaslavasky map [20]

The Zaslavasky map in two-dimension is defined as follows:

$$X_{n+1} = \text{mod}(X_n + \sigma(1 + \mu Y_n) + \omega \sigma \mu \cos(2\pi X_n), 1), \tag{2}$$

$$Y_{n+1} = e^{-\Phi}(Y_n + \omega \cos(2\pi X_n)) \tag{3}$$

$$\mu = \frac{1 - e^{-\Phi}}{\Phi} \tag{4}$$

Where the control parameters are  $\sigma$ ,  $\Phi$ , and  $\omega$ . The values for these parameters are:  $\sigma = 12.6695$ ,  $\Phi = 3.0$ ,  $\omega = 9.1$ .

The plot of the Zaslavasky map is shown in the figure below:

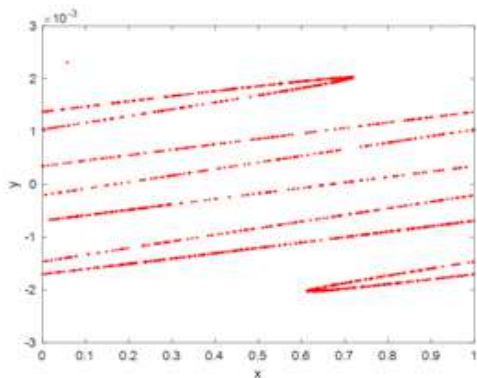


Fig. 2. Zaslavasky map phase diagram

C. Hénon Map [11]

The Hénon map has three dimensions (3D) in terms of system equations:

$$X_{n+1} = a - Y_n^2 - bZ_n \tag{5}$$

$$Y_{n+1} = X_n \tag{6}$$

$$Z_{n+1} = Y_n \tag{7}$$

This research employs  $a=1.76$  and  $b=0.1$ .

The chaotic attractor of the Hénon map is shown in the figure below:

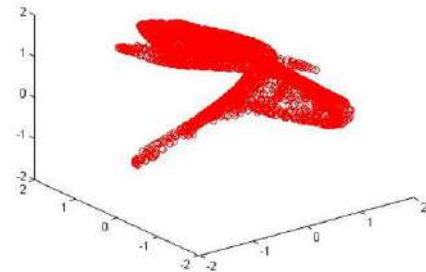


Fig. 3. 3D Hénon map chaotic attractor

IV. THE MOST SUITABLE SCHEME

The design was built on two pillars. To begin, an S-box was built using the Zaslavsky and Hénon maps. Second, by combining the values acquired by the equation of Logistic map with the equation of Hénon map, a hyperchaotic key sequence has been created. A hybrid form depending on the 3D Hénon map and the parameters of the Logistic map was used in the symmetric secret key manufacturing. The HyperLogVarHénon map sequence has been recorded as a matrix. Three identical matrices are generated from this matrix. Eventually, XOR has produced an encrypted image that serves as a lightweight transaction between the altered photo streams and the HyperLogVarHénon matrices created at random.

A. Generation of S-Box

The S-box employed in this suggestion is a combination of two chaotic maps, with the first half (128 elements) derived from a Zaslavsky map in two dimension and the second half (128 elements) derived from a Hénon map in three dimension. [11].

B. Scrambling Algorithm

The scrambling was done in two steps: first, the binary representation (bits) of each pixel was shuffled, and then, employing the S-box index (byte), the location of each pixel was scrambled. Fig. 4 shows the Scrambling mechanism. The  $m \times n \times 3$  input color image (i.e.  $256 \times 256 \times 3$ ) has been shuffled, then scaled to  $256 \times 256 \times 3$  pixels, and finally divided into channels red, green, and blue. The representation of each pixel value's decimal to binary was then converted. After that, each channel's bits were combined into only one vector. The vector has been divided into 16-bit discrete vectors. By substituting the first 4 values of the vectors (positions 1–4) with the final 4 values (positions 13–16), the first four values have been reversed. To create a single vector, the tiny vectors were

recombined. To retrieve the pixels' value, the binary information was translated to decimal representation for every eight bits. The vector has been divided into 256-bit tiny vectors. The proposed S-box's index was implemented to scramble each little vector value. A single scrambling vector was created by combining the scrambling of tiny vectors. To create a scrambling image, each changed channel was recombined. A scrambling image with a size of  $256 \times 256 \times 3$  has been created.

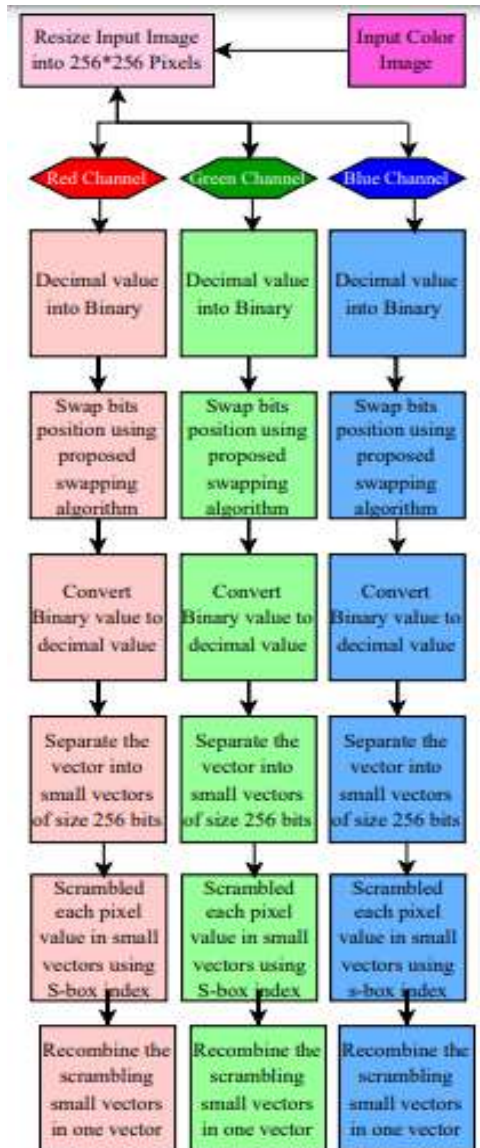


Fig. 4. The scrambling Design

### C. Encryption Algorithm

Fig. 5 depicts the encryption procedure algorithm. Calculating the value of image's 256 hyperchaotic matrix is the secret key for encrypting the scrambling color image using the Logistic and Hénon maps. The scrambling image is then encoded so that the keys of hyperchaotic matrix and the altering image matrix are processed using an XOR technique. A  $256 \times 256 \times 3$  pixel image has been distorted. The initial and parameter settings for the 1D Logistic map have been specified. The 3D Hénon map's initial parameter values have

been established, and the Logistic map sequence has been adopted as the major parameter values. According to the logistic equation (1), the location of the value created in a hybrid form was compared as follows:

- The output of logistic map in equation (6) is required by the value odd position in the chaotic chain.
- Using the logistic map's output in an equation (7) requires an even distribution of values in the chaotic sequence.

Afterward, the generating key sequence was saved in a HyperLogVarHénon map matrix with  $256 \times 256 \times 3$  values in length. The result sequence's keys have also been transformed to an unsigned number by duplicating elements in the width from 0 to 255 by 255. The value's constituents were then rounded to the nearest decimal value. As a consequence, the primary key sequence was generated using the obtained series. The matrix of HyperLogVarHénon map has been partitioned into three matrices, each having  $256 \times 256$  values in length, such that each channel has a key matrix. A  $256 \times 256$  scrambling color image I has been read.

The image was divided into three  $256 \times 256$  pixel red, green, and blue streams. XORs were employed to alter channels of the image utilizing randomly produced HyperLogVarHénon matrices that matched the actual dimensions of the source image. To mimic an encrypted image, the result has been transformed to a regular RGB value.

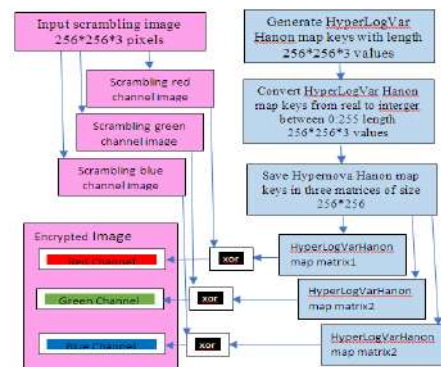


Fig. 5. Encrypting the scrambling color image

### D. Decryption Algorithm

The  $256 \times 256 \times 3$  encoded image is separated into red, green, and blue channels in this operation. Each encrypted image channel is XORed with the original image's HyperLogVarHénon matrices. The value of each pixel is translated from decimal to binary. Each channel's bits are merged into only one vector. The vector is broken down into small 16-bit vectors. By substituting the first 4 values of the vectors (positions 13–16) with the last 4 values (positions 1–4), the first four values are flipped. To create a specific vector, the tiny vectors are recombined. For every eight bits, the binary data is translated to decimal representation to acquire the pixels' value. The vector is broken down into discrete 256-bit vectors. The S-box index of the proposed S-box is used to decode each tiny vector value. Small vectors are descrambled and recombined to form a single scrambling vector. To create a descramble image, each changed channel is recombined. The  $256 \times 256 \times 3$  pixel descrambling image is saved.

V. EXPERIMENTAL RESULTS

To optimize the photo encryption approach efficiency, this section employed eight standard color images of size 256x256x3 as input digital photos. To demonstrate the experimental results, 8 sample photos (Lina, Baboon, Mona Liza, Peppers, Barbara, and Airplane) are used.

A. Key Space

Respect to current studies, if a cryptosystem's key space is larger than  $2^{100}$ , it can efficiently withstand modern computers' brute-force attacks [43]. As a consequence, the presented approach has appropriate key space to withstand brute-force attacks. The size of the key space of several chaos cryptography algorithms is listed in Table I.

TABLE I. Comparison Of Key Space of the Proposed Scheme With the Related Work.

Encoding scheme	Differnt algorithms				
	The Suitable algorithm	[46]	[58]	[29]	[22]
Key space	$2^{430}$	$2^{186}$	$2^{326}$	$2^{600}$	$2^{497}$

B. Correlation Coefficient Analysis

The coefficient of correlation of neighboring pixels is calculated using the formulas below [22,23,24]:

$$C_r = \frac{\text{cov}_{x,y}}{\sqrt{D_x} \sqrt{D_y}} \tag{8}$$

$$\text{cov}_{x,y} = \frac{1}{T} \sum_{i=1}^T (X_i - E(X))(Y_i - E(Y)), \tag{9}$$

$$E(X) = \frac{1}{T} \sum_{i=1}^T X_i, D(X) = \frac{1}{T} \sum_{i=1}^T (X_i - E(X))^2, \tag{10}$$

TABLE II. Image Correlation Coefficients

Image	Image Correlation Coefficients			
	Direction	Plain Image	Cipher Image	[24]
Lina	Horizontal	0.946001	0.003301	0.001201
Lina	Vertical	0.972003	0.007001	-0.00560
Lina	Diagonal	0.921201	0.002701	0.002702
Baboon	Horizontal	0.969402	0.002501	0.005401
Baboon	Vertical	0.963501	0.006401	.000601
Baboon	Diagonal	0.943701	0.003501	0.001801
Monaliza	Horizontal	0.993202	-0.00550	0.009601
Monaliza	Vertical	0.992701	0.005101	0.002701
Monaliza	Diagonal	0.986603	0.002201	0.001402
Peppers	Horizontal	0.971501	-0.00200	0.004001
Peppers	Vertical	0.977404	0.0000801	-0.00160
Peppers	Diagonal	0.947901	-0.006401	0.001502
Barbara	Horizontal	0.904101	-0.000050	-
Barbara	Vertical	0.925902	0.006101	-
Barbara	Diagonal	0.883002	0.001901	-
Airplane	Horizontal	0.904103	0.003402	-
Airplane	Vertical	0.925901	0.001301	-
Airplane	Diagonal	0.8830	0.0019	-

X, Y denote the two images' corresponding pixels, cov(x, y), E(x), and D(x) denote covariance, mean, and variance, respectively, and T is the overall amount of pixels in the image. To demonstrate the correlation of nearby pixels, Fig. 6 displays the correlations in horizontal, vertical, and diagonal

direction of the Lina unmasked and cipher images using the suggested encryption technique. The results are summarized in Table II.

C. Histogram Analysis[29]

The histograms for numerous photos, including the decoding image, are shown in Fig.7. Because the pixels in the decoding images are equally scattered, each level of intensity has occurrence probability that is closer to the equivalent.

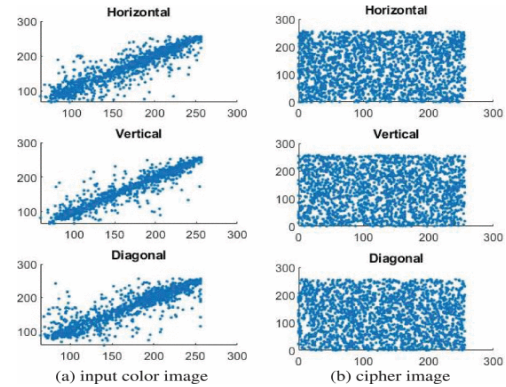


Fig. 6. The correlation coefficient analysis.

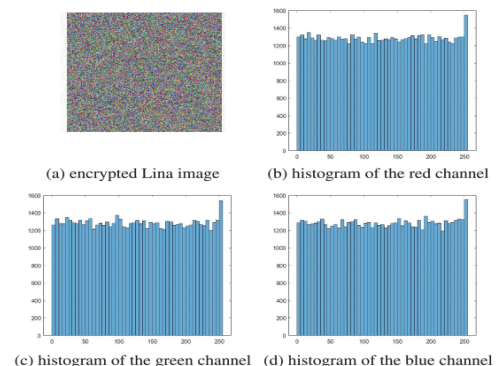


Fig. 7. Histogram analysis

D. Sensitivity to Security Keys[33]

The metrics of NPCR and UACI analyzed between the plain photo and the encoded photo with the adjusted key are shown in Table III. The test was conducted using the Lina image. The findings show that a little change in the values of security keys generates indistinguishable randomized images from instructional items.

TABLE III. Result Of Key Sensitivity (Uses Lina Image)

Key	Key Sensitivity Result Using Lina Image					
	$C=4 \times 10^{-2}$	$\beta=\beta \times 10^{-12}$	$\Gamma=\Gamma \times 10^{-12}$	$\alpha=\alpha \times 10^{-12}$	$a=a \times 10^{-12}$	$b=b \times 10^{-12}$
NPCR	99.5941	99.6002	99.5956	99.59411	99.6205	99.58445
	1	1	4		6	
UACI	30.4664	30.3924	30.3674	30.51093	30.4505	30.37768
	2	4	7		4	

E. Information Entropy Analysis[38]

Table IV displays the entropy of information of the three-color pixel streams, and the values obtained are all near to 8. The values of entropy of various encryption algorithms are shown in Table V. Furthermore, the research reveals that the

encryption approach may approximate the encryption of a random image.

TABLE IV. Information Entropy Result

Information Entropy Result	Image Name					
	Lina	Baboon	Monaliza	Peppers	Barbara	Airplane
Plain Image Entropy	7.75994	7.61280	7.38081	7.77491	7.64546	6.79310
Cipher Image Entropy	7.99918	7.99907	7.99910	7.99890	7.99910	7.99904

TABLE V. Comparison of Entropy With Another Scheme

Different Entropy	Encrypted Scheme					
	The Suitable Algorithm	[58]	[24]	[29]	[22]	[51]
Entropy	7.99913	7.99750	7.94368	7.90263	7.99716	7.9987
Peppers Entropy	7.99903	7.9973	7.95264	7.9999	7.99735	7.9987
Baboon Entropy	7.99911	7.9970	7.98655	7.9999	-	7.9988

F. Speed Analysis and Complexity[46]

Table VI shows the estimated time for different photos relying on the time of encoding and decoding of color images of size 256x256. Table VII compares the speed of the suggested encryption with the speed of the most commonly used reference methods.

TABLE VI. Time of Encoding and Decoding

Operation	Image Name					
	Lina	Baboon	Monaliza	Peppers	Barbara	Airplane
Encryption Time	0.349301	0.349501	0.352501	0.349301	0.304001	0.301101
Decryption Time	0.441101	0.391001	0.399201	0.417901	0.410101	0.400201

TABLE VII. Analysis Of Speed of Proposed Encryption with Alternative Reference Strategies. (Using Lina Image)

Operation	Different Schemes			
	The Suitable algorithm	[46]	[42]	[29]
Encoding stage (s)	0.39301	0.4212501	1.061201	0.831401
Decoding Stage (s)	0.441101	2.1274001	1.629101	4.253101

G. Differential Attack Analysis[51]

Table VIII indicates that the performance of opposing diverse attacks was examined using three color photos, and the data reveal that the chosen scheme is heavily dependent on the input plain photo to cope with differential attacks. Although the value of NPCR is larger than 95%, the value of UACI is larger than 33%. As seen in Tables VIII and IX, the chosen scheme is quite sensitive to the plain photo when interacting with differential attacks.

TABLE VIII. Results of NPCR and UACI of Cipher Images

Results	Image Name					
	Lina	Baboon	Monaliza	Peppers	Barbara	Airplane
NPCR	99.61937001	99.62361001	99.61344001	99.60937001	99.62158001	99.61344001
UACI	33.44153001	33.82484001	33.98317001	33.83490001	33.46354001	33.55539001

TABLE IX. Comparison of the NPCR and UACI Values of the Lina (256x256) Image.

Results	References					
	The Suitable Scheme	[58]	[24]	[29]	[22]	[51]
NPCR	99.619401	99.6001	99.6301	99.6201	99.596501	99.5901
UACI	33.441501	30.334801	30.5101	33.5201	33.458801	30.9701

H. Noise Attack Analysis

PSNR can be calculated using the following formula [58] to determine the decrypted image's quality after the assault:

$$PSNR = 10 \times \log_{10} \left( \frac{Max_1}{\sqrt{MSE}} \right) \tag{11}$$

$$MSE = \frac{1}{qp} \sum_{j=0}^{q-1} \sum_{k=0}^{p-1} \|M(j,k) - N(j,k)\|^2 \tag{12}$$

MSE is the mean squared error between the plain and produced images, Max is the maximum image point color value, showing M(j,k), N(j,k) pixel values for the source and restored images, respectively. The value of PSNR between the encoded and plain photos is computed and presented in Table X.

TABLE X. Quantitative Measurement of different Noises

Attack Resistance	Noise Type					
	Gaussian Noise	Gaussian Noise	Gaussian Noise	Gaussian Noise	Salt and pepper Noise	Salt and pepper Noise
Noise Intensity	0.000501	0.0050	0.0500	0.0005	0.0050	0.0501
PSNR In The Suitable Algorithm	20.210301	20.197001	19.34010101	37.255101	28.271301	18.079201
PSNR In [29]	20.223001	20.196401	19.37100101	38.580201	27.957801	18.126101

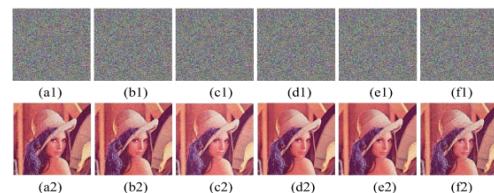


Fig. 8(a1) Cipher image under 0.0005 Gaussian noise, (b1) Cipher image under 0.005 Gaussian noise, (c1) Cipher image under 0.05 Gaussian Noise, (d1) Cipher image under 0.0005 Salt and Pepper noise, (e1) Cipher image under 0.005 Salt and Pepper noise, (f1) Cipher image under 0.05 Salt and Pepper noise, (a2) Decipher image under 0.0005 Gaussian noise, (b2) Decipher image under 0.005 Gaussian noise, (c2) Decipher image under 0.05 Gaussian noise, (d2) Decipher image under 0.0005 Salt and Pepper noise, (e2) Decipher image under 0.005 Salt and Pepper noise, (f2) Decipher image under 0.05 Salt and Pepper noise.

REFERENCES

[1] "The Wolf Prize in Physics in 1986". Archived from the original on 2012-02-05. Retrieved 2008-01-17.  
 [2] Nasry, Hany & Abdallah, Azhaar & Farhan, Alaa & Ahmed, Hossam & Alsobky, Wageda. (2022). Multi Chaotic System to Generate Novel S-Box for Image Encryption. Journal of Physics: Conference Series. 2304. 012007. 10.1088/1742-6596/2304/1/012007.

- [3] Abd-Elhalim Zikry, Hossam Labib Zayed, Fatima Newagy, and Salih Hssan Mahmood, "Effect of Switching Loads on The Power Line Communication (PLC) Modems Inside Diret Local Area Network (DLAN) ", Al-Azhar Engineering Thirteenth International Conference(AEIC 2014), Cairo, Egypt, December 23-25,2014.
- [4] Galal, M. E. A. Ibrahim and H. E. Ahmed, "Exploring frequency tuning policies for USRP-N210 SDR platform and GNU radio," 2013 Conference on Design and Architectures for Signal and Image Processing, 2013, pp. 298-303.
- [5] Mohamed G Abd Elfatah, Hany Nasry Zaky and Ahmed Shams" Mobile Robot Position Estimation using Milstein Algorithm" Journal of Physics: Conference Series, Volume 1970, 10th International Conference on Mathematics and Engineering Physics (ICMEP-10), 7-9 April 2020, Military Technical College, Kobry El-Kobbah, Cairo, Egypt
- [6] Wang, Xingyuan; Zhao, Jianfeng (2012). "An improved key agreement protocol based on chaos". Commun. Nonlinear Sci. Numer. Simul. 15 (12): 4052–4057.
- [7] W. I. El Sobky, A. R. Mahmoud, A. S. Mohra and T. El-Garf, "Enhancing Hierocrypt-3 performance by modifying its S-Box and modes of operations," Journal of Communications, pp. 905-912.
- [8] El-Meligy, N. E., Diab, T. O., Mohra, A. S., Hassan, A. Y., & El-Sobky, W. I. (2022). A Novel Dynamic Mathematical Model Applied in Hash Function Based on DNA Algorithm and Chaotic Maps. Mathematics, 10(8), 1333.
- [9] D. Riadh and R. Shaker, "Implementation of gray image encryption using multi-level of permutation and substitution", Int. J. Appl. Inf. Syst., vol. 10, no. 1, pp. 25-30, Nov. 2015.
- [10] Z. A. Abduljabbar et al., "Provably Secure and Fast Color Image Encryption Algorithm Based on S-Boxes and Hyperchaotic Map," in IEEE Access, vol. 10, pp. 26257-26270, 2022, doi: 10.1109/ACCESS.2022.3151174.
- [11] S. Ibrahim and A. Alharbi, "Efficient image encryption scheme using Henon map dynamic S-boxes and elliptic curve cryptography", IEEE Access, vol. 8, pp. 194289-194302, 2020.
- [12] L. Qiao and K. Nahrstedt, "Comparison of mpeg encryption algorithms," Computers and Graphics, vol. 22, no. 4, pp. 437-448, 1998.
- [13] H. Nasry, Chunlan Ye, Jianwei Gong, and Huiyan Chen, "Time-Delay Compensation in Environment Construction Using Laser Range Finder", vol.5, pp. 707-711, Aug. 2013. DOI: 10.7763/IJCTE.2013.V5.780
- [14] Kadir A, Aili M, Sattar M (2017) Color image encryption scheme using coupled hyper chaotic system with multiple impulse injections. Opt Int J Light Electron Opt 129:231–238
- [15] Irani BY, Ayubi P, Jabalkandi FA, Valandar MY, Barani MJ (2019) Digital image scrambling based on a new one-dimensional coupled Sine map. Nonlinear Dyn 97(4):2693–2721
- [16] Liu H, Wen F, Kadir A (2019) Construction of a new 2D Chebyshev-Sine map and its application to color image encryption. Multimed Tools Appl 78(12):15997–16010
- [17] Niyat AY, Moattar MH, Torshiz MN (2017) Color image encryption based on hybrid hyper-chaotic system and cellular automata. Opt Lasers Eng 90:225–237
- [18] Pak C, Huang L (2017) A new color image encryption using combination of the 1D chaotic map. Signal Process 138:129–137
- [19] T. Li, J. Shi and D. Zhang, "Color image encryption based on joint permutation and diffusion", Proc. SPIE, vol. 30, no. 1, Feb. 2021.
- [20] R. Hamza and F. Titouna, "A novel sensitive image encryption algorithm based on the Zaslavsky chaotic map", Inf. Secur. J., vol. 25, no. 4, pp. 162-179, 2016.
- [21] Ahmed S. Abdelwahed, Abdel Halim Zekry, Hossam Labib Zayed, and Ahmed M. Sayed "Controlling Electricity Consumption At Home Smart home", IEEE Tenth International Conference on Computer Engineering & Systems (ICCES), Cairo, Egypt, pp. 49-54, December 23-24, 2015.
- [22] X. Wang, Y. Wang, X. Zhu and C. Luo, "A novel chaotic algorithm for image encryption utilizing one-time pad based on pixel level and DNA level", Opt. Lasers Eng., vol. 125, Feb. 2020.
- [23] H. A. M. A. Basha, A. S. S. Mohra, T. O. M. Diab and W. I. E. Sobky, "Efficient Image Encryption Based on New Substitution Box Using DNA Coding and Bent Function," in IEEE Access, vol. 10, pp. 66409-66429, 2022, doi: 10.1109/ACCESS.2022.3183990.
- [24] H. M. Al-Mashhadi and I. Q. Abduljaleel, "Color image encryption using chaotic maps triangular scrambling with DNA sequences," 2017 International Conference on Current Research in Computer Science and Information Technology (ICCCIT), 2017, pp. 93-98, doi: 10.1109/ICCCIT.2017.7965540.
- [25] I. Galal, M. E. A. Ibrahim, H. E. Ahmed and A. Zekry, "Performance evaluation of digital modulation techniques used in Bluetooth physical/radio layer," 2012 Seventh International Conference on Computer Engineering & Systems (ICCES), 2012, pp. 1-7, doi: 10.1109/ICCES.2012.6408477.
- [26] J. Scharinger, "Fast encryption of image data using chaotic Kolmogorov flows," Journal of Electronic Imaging, vol. 7, no. 2, pp. 318–325, 1998.
- [27] Aly A.E. Elwazan, Abdelhalim A. A. Zekry, and Hossam L. A.Zayed, "Matlab Code for LTE Convolutional Code and Viterbi Decoder", International Journal of Engineering Research & Technology (IJERT), ISSN: 2278-0181, Vol. 6 Issue 03, March-2017.
- [28] A. Mansour, Z. Chengning and H. Nasry, "Measurement of power components in balanced and unbalanced three-phase systems under nonsinusoidal operating conditions by using IEEE standard 1459–2010 and Fourier analysis," 2013 The International Conference on Technological Advances in Electrical, Electronics and Computer Engineering (TAEECE), 2013, pp. 166-171, doi: 10.1109/TAEECE.2013.6557216.
- [29] X. Qian, Q. Yang, Q. Li, Q. Li, Y. Wu and W. Wang, "A novel color image encryption algorithm based on three-dimensional chaotic maps and reconstruction techniques", IEEE Access, vol. 9, pp. 61334-61345, 2021.
- [30] M. E. A. Ibrahim and H. E. Ahmed, "Embedded SDR implementation for wireless frequency hopping transceiver," The 2011 International Conference on Computer Engineering & Systems, 2011, pp. 167-172, doi: 10.1109/ICCES.2011.6141034.
- [31] A. K. A. Hassan, "Proposed hyperchaotic system for image encryption", Int. J. Adv. Comput. Sci. Appl., vol. 7, no. 1, pp. 15-27, 2016.
- [32] B. Li, J. Gong, Y. Jiang, H. Nasry and G. Xiong, "ARA\*+: Improved Path Planning Algorithm Based on ARA\*," 2012 IEEE/WIC/ACM International Conferences on Web Intelligence and Intelligent Agent Technology, 2012, pp. 361-365, doi: 10.1109/WI-IAT.2012.13.
- [33] Y. Mao and G. Chen, "Chaos based image encryption," in Handbook of Computational Geometry for Pattern Recognition, Computer Vision, Neural Computing and Robotics, E. B. Corrochano, Ed., Springer, Heidelberg, Germany, 2004.
- [34] Eman Gaber Ahmed Mahmud, Hosamlabib, Ashraf Mohamed Ali Hassen, and Amin Mohamed Nasser "Adaptive Resource Management Strategy with Multi-Service in Heterogeneous Networks", IOSR Journal of Electronics and Communication Engineering (IOSR-JECE) e-ISSN: 2278-2834,p- ISSN: 2278-8735. Volume 12, Issue 4, Ver. V (Jul.-Aug. 2017), PP 41-44.
- [35] Nasry, Hany. (2019). Coordinate Transformation in Unmanned Systems Using Clifford Algebra. ICMRE'19: Proceedings of the 5th International Conference on Mechatronics and Robotics Engineering. 167-170. 10.1145/3314493.3314496.
- [36] Ahmed, H. E., Zekry, A. A., Elhennawy, A. E., & Hassan, A. M. (2010). DSP Implementation Aspects for a Generic Frequency Hopped Transceiver.
- [37] A. M. Mahfouz, A. S. Ismail, H. Nasry and W. I. Elsobky, "Path Detection for A Moving Target in Wireless Sensor Network Based on Clifford Algebra," 2022 International Telecommunications Conference (ITC-Egypt), 2022, pp. 1-5, doi: 10.1109/ITC-Egypt 55520.2022.9855765.
- [38] N. Iqbal, R. A. Naqvi, M. Atif, M. A. Khan, M. Hanif, S. Abbas, et al., "On the image encryption algorithm based on the chaotic system DNA encoding and castle", IEEE Access, vol. 9, pp. 118253-118270, 2021.
- [39] Ezzeddine Touti, Hossem Zayed, Remus Pusca and Raphael Romary "Dynamic Stability Enhancement of a Hybrid Renewable Energy System in Stand-Alone Applications ", Computation 2021, 9, 14. https://doi.org/10.3390/computation9020014 , February 2021.
- [40] Eman Salem , Abdelhalim Zekry, Hossam Labebe, and Radwa Tawfik "FPGA implementation of 1000base-x Ethernet physical layer core", International Journal of Engineering & Technology (IJET), 7 (4) (2018) PP 2106-2112.
- [41] Zaky, Hany & Ismail, Ahmed. (2018). Mathematical Model for UGV Transparency Using Laser Range Finder. The International Conference on Mathematics and Engineering Physics. 9. 1-6. 10.21608/icmep.2018.29419.

- [42] A. M. Asl, A. Broumandnia, and S. J. Mirabedini, "Scale invariant digital color image encryption using a 3D modular chaotic map," IEEE Access, vol. 9, pp. 102433–102449, 2021.
- [43] Alsobky, W., Saeed, H., & Elwakeil, A. N. (2020). Different Types of Attacks on Block Ciphers. *Int. J. Recent Technol. Eng.*, 9(3), 28-31.
- [44] Khaled Abu-Bakr Nigm, Ahmed K Elsherif and Ahmed Salah Ismail. Fuzzy Estimation of the Mean for Electric Load Consumption Based on Different Algorithms. IOP Conference Series: 610, (ASAT-18) 2019. <https://doi.org/10.1088/1757-899X/610/1/012011>
- [45] Abd Elfatah, Mohamed & Zaky, Hany & Gharib, M. (2019). Mobile robot position estimation using Euler-Maruyama algorithm. IOP Conference Series: Materials Science and Engineering. 610. 012074. [10.1088/1757-899X/610/1/012074](https://doi.org/10.1088/1757-899X/610/1/012074).
- [46] T. Li, J. Shi, and D. Zhang, "Color image encryption based on joint permutation and diffusion," Proc. SPIE, vol. 30, no. 1, Feb. 2021, Art. no. 013008.
- [47] T. O. Diab and A. M. Darwish, "A new linear model for image representation for use with Kalman filter restoration," 2000 10th European Signal Processing Conference, 2000, pp. 1-4.
- [48] Elsayed, M. M., Khalil, A. T., Diab, T. O. M., & Mohra, A. S. S. S. (2018). Hybrid method for brain tumor extraction and MRI scan classification. *International Journal of Engineering & Technology*, 7(4), 4769-4779.
- [49] Eladawi, Ahmad E., Tamer O. Diab, and Hammad T. Elmetwally. "Forming Temperature Investigation of Aluminum and Aluminum/Silicon Carbide Using Image Texture Features." *Machining, Joining and Modifications of Advanced Materials*. Springer, Singapore, 2016. 33-44.
- [50] Eladawi, A. E., Sayed, S. A., Elmetwally, H. T., & Diab, T. O. (2017). Prediction of Strain Rate of Aluminum/Silicon Carbide Using Gray Level Run-Length Matrices. *Journal of Energy and Power Engineering*, 11, 355-361.
- [51] I. Q. Abduljaleel, S. A. Abdul-Ghani and H. Z. Naji, "An image of encryption algorithm using graph theory and speech signal key generation", *J. Phys. Conf. Ser.*, vol. 1804, no. 1, Feb. 2021.
- [52] Nasry, Hany, Wei Xu, Jian Wei Gong, and Hui Yan Chen. "Teleoperation Transparency Using Model Predictive Control." *Applied Mechanics and Materials*. Trans Tech Publications, Ltd., November 2013. <https://doi.org/10.4028/www.scientific.net/amm.446-447.1151>.
- [53] M. Mansour, W. Elsobky, A. Hasan and W. Anis, "Appraisal of Multiple AES Modes Behavior using Traditional and Enhanced Substitution Boxes," *International Journal of Recent Technology and Engineering*, vol. 8, no. 5, pp. 530-539, 2020.
- [54] E. W. Afify, R. Abo Alez, A. T. Khalil and W. I. Alsobky, "Performance Analysis of Advanced Encryption Standard (AES) S-boxes," *International Journal of Recent Technology and Engineering*, vol. 9, no. 1, pp. 2214-2218, 2020.
- [55] E. W. Afify, R. Abo Alez, A. T. Khalil and W. I. Alsobky, "Algebraic Construction of Powerful Substitution Box," *International Journal of Recent Technology and Engineering*, vol. 8, no. 6, pp. 405-409, 2020.
- [56] Mahfouz, Amr & Nasry, Hany & Ismail, Ahmed & Dahab, Eiman. (2022). Mathematical Model for Omnidirectional Sensor Network Using Clifford Algebra. *Journal of Physics: Conference Series*. 2304. 012001. [10.1088/1742-6596/2304/1/012001](https://doi.org/10.1088/1742-6596/2304/1/012001).
- [57] Khaled Abu-Bakr Nigm, Ahmed K Elsherif and Ahmed Salah Ismail. Error Analysis between Two Different Fuzzy Multiplication Operations on Triangular Fuzzy Number. *Journal of Physics: Conference Series*, 1970, (ICMEP-10), 2020. <https://doi.org/10.1088/1742-6596/1970/1/012003>
- [58] S. Zhou, P. He, and N. Kasabov, "A dynamic dna color image encryption method based on SHA-512," *Entropy*, vol. 22, no. 10, pp. 964–975, 2020.
- [59] Khaled Abu-Bakr Nigm, Ahmed Salah Ismail and Ahmed K Elsherif. Fuzzy Estimation for the Difference between Two Means using Different Algorithms. *Journal of Physics: Conference Series*, 1970, (ICMEP-10), 2020. <https://doi.org/10.1088/1742-6596/1970/1/012004>